applied sciences

MDPI

Article

Stability of Traffic Equilibria in a Day-to-Day Dynamic Model of Route Choice and Adaptive Signal Control

Claudio Meneguzzer

Department of Civil, Environmental and Architectural Engineering, University of Padova, Via Marzolo 9, 35131 Padova, Italy; claudio.meneguzzer@unipd.it

Abstract: Adaptive traffic signal control has the potential to promote the efficient use of road intersections, thus contributing to the effectiveness of urban traffic management schemes. However, the reaction of drivers to repeatedly updated signal settings and the ensuing route choice dynamics may trigger the emergence of various kinds of network instability. In this study, the joint evolution of traffic flows and adaptive signal settings in a road network is investigated at the level of day-to-day dynamics with an explicit focus on the stability issue. We show how a Logit form signal control policy can be used, in interaction with route choice, to counter the emergence of instabilities possibly arising as a consequence of various behavioral factors and network conditions. After providing a general formulation of the model as a discrete time, deterministic nonlinear dynamical system, an explicit analysis of fixed-point stability is carried out for a simple network. Numerical results obtained from the implementation of the model on two example networks are presented in order to support the analytical findings of this study. We conclude that, in an integrated traffic management and information system, a properly calibrated adaptive signal control policy has the potential to offset the destabilizing effect of highly accurate driver information supplied by navigational aids. Our findings also suggest that the Logit-like control policy performs better than the Equisaturation signal setting method, in terms of average intersection delay at equilibrium, for all levels of driver information and travel demand tested in the experiment.

Keywords: transportation networks; traffic assignment; route choice; road intersections; signal control; intersection delay; day-to-day dynamics; nonlinear dynamical system; fixed-point stability

Citation: Meneguzzer, C. Stability of Traffic Equilibria in a Day-to-Day Dynamic Model of Route Choice and Adaptive Signal Control. *Appl. Sci.* **2024**, *14*, 1891. https://doi.org/10.3390/app14051891

Academic Editors: Abdeljalil Abbas-Turki, Mahjoub Dridi and Yazan Mualla

Received: 4 February 2024
Revised: 21 February 2024
Accepted: 22 February 2024
Published: 25 February 2024

1. Introduction and Background

Signal control plays a key role in promoting the efficient use of physical capacities of road intersections and is considered an essential tool for traffic management in urban networks. Technological advancements in both hardware and software have fostered the evolution from the fixed-time operation of traffic lights to sophisticated forms of adaptive signal control, allowing the signal plan to respond, at various time scales, to the fluctuations of intersection traffic demands.

The possibility of continuously updating signal settings in response to the variations of traffic flows leads quite naturally to the emergence of a mutual interaction between route choices and signal control. Traffic assignment models taking explicitly into account such mutual dependence are then needed to ensure realistic and policy-sensitive forecasts of network flows. Allsop [1] is commonly believed to have been the first to recognize the importance of combining traffic assignment and signal control into a single modeling framework, in which both route choices and signal settings are treated as endogenous variables. The development and implementation of such an integrated approach raises a number of interesting analytical and computational issues, making these combined models more challenging as compared to conventional route choice models [2,3].

While the original focus of combined traffic assignment and control models was on the analysis and computation of mutually consistent route choices and signal settings

from an equilibrium perspective [4–7], the emphasis of more recent research efforts has shifted toward the joint modeling of adaptive signal control and day-to-day route choice dynamics [8–10].

The day-to-day dynamic approach to route choice modeling, pioneered by the works of Horowitz [11] and Smith [12], realistically recognizes that the temporal evolution of network states does not necessarily converge to equilibrium conditions but may rather lead to other types of long-term outcomes, such as periodic or aperiodic attractors. The theoretical and practical relevance of day-to-day assignment models is further substantiated by their close connection with the issue of stability and the analysis of attraction domains of traffic equilibria [13–16]. More recently, the day-to-day dynamic approach has been adopted for the simulation of route choice in the context of cutting-edge traffic scenarios, such as the operation of a road network used by mixed flows of autonomous and human-driven vehicles [17]. The effects of specific behavioral traits of travelers on the evolution of network states have also been modeled within a day-to-day dynamic framework [18]. Parallel to the stream of studies addressing the theoretical aspects of day-to-day traffic dynamics, an active area of research dealing with the empirical analysis of repeated route choice behavior in real or simulated settings has developed [19–23].

The study of the joint dynamics of day-to-day route choice and adaptive signal control under real-time information was addressed by Hu and Mahmassani [24] through a simulation and assignment procedure. Numerical experiments were carried out by the authors in order to compare the effectiveness of different combinations of signal control strategies and levels of information availability.

Cantarella [8] presented a formal definition of the combined day-to-day signal control and traffic assignment problem based on a discrete time, deterministic process model with exponentially smoothed cost and flow updating rules. He provided fixed-point stability conditions considering different approaches to the determination of signal settings. Related works by Cantarella et al. [25,26] showed how equilibrium stability conditions can be embedded as a constraint in a day-to-day signal setting–route choice framework and demonstrated the applicability of the resulting model to a realistic size network.

Meneguzzer [9] showed that the frequency of signal updating may significantly affect the duration of the day-to-day dynamic process needed to achieve a network flow–control equilibrium and provided examples of bifurcations arising as a result of model parameters crossing certain critical thresholds. Xiao and Lo [10] investigated the behavior of a joint route choice–signal control dynamical system and illustrated the computation of fixed points through a simple three-link network example. They also demonstrated how the knowledge of the attraction domains of different fixed points can be instrumental in defining an appropriate adaptive signal control scheme.

Smith [27] proposed a dynamical system model of the day-to-day evolution of route flows, bottleneck delays, and signal green times based on the proportional switch adjustment process [12] and on an extension of the so-called P_0 control policy [28,29]. He showed that, under the assumption of vertical queuing, the dynamical system is convergent and network capacity is maximized.

Liu and Smith [30] analyzed the stability of a day-to-day dynamic model of route choice and signal control based on flow swaps between paired alternative segments [31] and used red times as signal control variables. Smith et al. [32] studied the properties of some "pressure driven" responsive control policies within dynamical models of route choice and signal control, while Smith et al. [33] demonstrated the potential of a coordinated implementation of signal control and pricing for eliminating queues and maximizing network throughput.

He et al. [34] proposed a discrete time optimal control formulation of the day-to-day signal retiming problem for single-destination networks using a traffic flow evolution model based on splitting rates at nodes [35]. Shang et al. [36] applied adaptive signal control in combination with day-to-day route choice dynamics and deep reinforcement

learning as a traffic management strategy aimed at improving the resilience of urban road networks under disruptions in emergency situations.

Among the many modeling and implementation aspects of the day-to-day dynamics of route choice and signal control, the issue of equilibrium stability deserves special attention. A stable network equilibrium represents a consistent reference state, whose prediction can provide a sound and reliable basis for design and management activities. The relevance of this concept provides the motivation for the work described in this paper, whose main aim is to show how a properly calibrated signal control policy can be used, in a day-to-day dynamic framework, to protect the system from instabilities triggered by other factors and conditions.

The remainder of the paper is organized as follows. In Section 2, the general formulation of the dynamic process model describing the joint evolution of route choices and signal settings is presented, and explicit fixed-point stability conditions are derived for a two-link network. The results of numerical tests of the proposed model are illustrated in Section 3 for a two-link network and in Section 4 for a grid network. Concluding remarks and suggestions for possible developments of the proposed approach are offered in Section 5.

2. Method

2.1. General Formulation of the Problem

We consider a road network in which intersections are controlled by adaptive traffic signals. The day-to-day evolution of states of such a network can be described by means of a discrete time, deterministic process model formulated in terms of link variables as follows [8]:

$$\boldsymbol{C}^t = \beta \boldsymbol{K}\left(\boldsymbol{F}^{t-1}, \boldsymbol{G}^{t-1}\right) + (1-\beta)\boldsymbol{C}^{t-1} \tag{1}$$

$$\boldsymbol{F}^t = \alpha \boldsymbol{S}\left(\boldsymbol{C}^t\right) + (1-\alpha)\boldsymbol{F}^{t-1} \tag{2}$$

$$\boldsymbol{G}^t = \boldsymbol{H}\left(\boldsymbol{F}^t\right) \tag{3}$$

where

t represents the generic period ("day") of the dynamic process;
$\boldsymbol{C}^t$ is the vector of mean perceived link costs at the start of day t;
$\boldsymbol{F}^t$ is the vector of link flows on day t;
$\boldsymbol{G}^t$ is the vector of signal settings on day t;
$\boldsymbol{K}$ is the vector representing average link costs actually experienced by users as a function of link flows and signal settings;
$\boldsymbol{S}$ is the vector function representing the relationship between link flows and mean perceived link costs based on an assumed probabilistic route choice model;
$\boldsymbol{H}$ is the vector function representing the relationship between signal settings and link flows based on an assumed signal control policy;
β $(0 < \beta \leq 1)$ is a parameter quantifying the extent to which the most recent travel experience ("yesterday's trip") contributes to the formation of the cost perceived by users at the start of day t;
α $(0 < \alpha \leq 1)$ is a parameter representing the fraction of travelers who actually reconsider their previous day's choice.

Note that parameter β controls the rate at which perceived costs are updated as a consequence of the previous day's experience, and hence it allows us to represent the effect of memory and learning on drivers' route choice behavior. In the limit, when $\beta = 1$, travelers are "memoryless", as they base their next choice solely on the most recently experienced costs. On the other hand, parameter α controls the extent to which route choices are adjusted in response to updated costs. It allows us to represent the effect of habit and inertia on drivers' behavior, as $(1-\alpha)$ represents the fraction of users who repeat their previous day's choice, regardless of the cost actually experienced. Note that when

$\alpha = 1$, all drivers are "inertia-free", as they reconsider their route choices on a daily basis without any habit effect.

Substituting Equation (1) for $\boldsymbol{C}^t$ in Equation (2) and expressing the signal settings through the signal control policy (3), model (1)–(3) can be reformulated as the following nonlinear dynamical system:

$$\boldsymbol{C}^t = \beta \boldsymbol{K}\left[\boldsymbol{F}^{t-1}, \boldsymbol{H}\left(\boldsymbol{F}^{t-1}\right)\right] + (1-\beta)\boldsymbol{C}^{t-1} \tag{4}$$

$$\boldsymbol{F}^t = \alpha \boldsymbol{S}\left\{\beta \boldsymbol{K}\left[\boldsymbol{F}^{t-1}, \boldsymbol{H}\left(\boldsymbol{F}^{t-1}\right)\right] + (1-\beta)\boldsymbol{C}^{t-1}\right\} + (1-\alpha)\boldsymbol{F}^{t-1} \tag{5}$$

whose fixed points $(\widetilde{\boldsymbol{C}}, \widetilde{\boldsymbol{F}})$ are found by setting

$$\boldsymbol{C}^t = \boldsymbol{C}^{t-1} = \widetilde{\boldsymbol{C}} \tag{6}$$

$$\boldsymbol{F}^t = \boldsymbol{F}^{t-1} = \widetilde{\boldsymbol{F}} \tag{7}$$

which yields

$$\widetilde{\boldsymbol{C}} = \boldsymbol{K}\left[\widetilde{\boldsymbol{F}}, \boldsymbol{H}(\widetilde{\boldsymbol{F}})\right] \tag{8}$$

$$\widetilde{\boldsymbol{F}} = \boldsymbol{S}(\widetilde{\boldsymbol{C}}) \tag{9}$$

and the fixed-point signal settings are given by

$$\widetilde{\boldsymbol{G}} = \boldsymbol{H}(\widetilde{\boldsymbol{F}}) \tag{10}$$

According to a basic result of nonlinear dynamical systems theory, a fixed point $(\widetilde{\boldsymbol{C}}, \widetilde{\boldsymbol{F}})$ is locally stable if all eigenvalues of the Jacobian matrix of (4) and (5), evaluated at $(\widetilde{\boldsymbol{C}}, \widetilde{\boldsymbol{F}})$, have a modulus smaller than 1. Explicit analytical expressions ensuing from this condition are derived in the following subsections for the case of a simple two-link network.

2.2. Day-to-Day Dynamics of Route Choice and Signal Control in a Two-Link Network

We consider a two-link road network connecting a single Origin–Destination (O-D) pair with a total travel demand of 1 unit. The two links intersect at some point before reaching the destination, as shown in Figure 1. As a result of flow conservation, the flow pattern is uniquely determined by the value of a single variable; in what follows, we denote F as the flow on link 1 and $(1 - F)$ as the flow on link 2. The intersection between the two links is controlled by a two-phase traffic signal operating with a fixed and given cycle length. For the sake of simplicity, lost times occurring during phase transitions are not considered, and minimum/maximum green splits are not enforced. The state of the traffic signal can thus be identified by the value of one of the two green splits; in what follows, we denote G as the green split assigned to link 1 and $(1 - G)$ as the green split assigned to link 2.

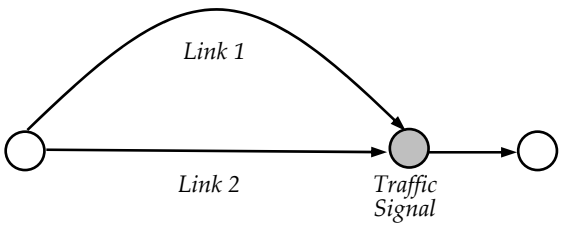

Figure 1. Two-link network with a signal-controlled intersection.

Based on the above assumptions, expressions (1)–(3) can be rewritten in scalar form as follows:

$$C_1^t = \beta K_1\left(F^{t-1}, G^{t-1}\right) + (1-\beta)C_1^{t-1} \tag{11}$$

$$C_2^t = \beta K_2\left(1-F^{t-1}, 1-G^{t-1}\right) + (1-\beta)C_2^{t-1} \tag{12}$$

$$F^t = \alpha S\left(C_1^t - C_2^t\right) + (1-\alpha)F^{t-1} \tag{13}$$

$$G^t = H\left(F^t\right) \tag{14}$$

where we note that, according to (13), the fraction of "habit-free" drivers choosing link 1 on day t is expressed as a function of the difference between the perceived costs of the two links on day t.

Next, we define $Z = C_1 - C_2$ and $V(F,G) = K_1(F,G) - K_2(1-F, 1-G)$ and subtract (12) from (11), so that (11)–(13) are reduced to the following expressions:

$$Z^t = \beta V\left(F^{t-1}, G^{t-1}\right) + (1-\beta)Z^{t-1} \tag{15}$$

$$F^t = \alpha S\left(Z^t\right) + (1-\alpha)F^{t-1} \tag{16}$$

Substituting Equation (15) for Z^t into (16) and expressing G via the signal control policy (14), we obtain the following two-dimensional nonlinear dynamical system:

$$Z^t = \beta V\left[F^{t-1}, H\left(F^{t-1}\right)\right] + (1-\beta)Z^{t-1} \tag{17}$$

$$F^t = \alpha S\left\{\beta V\left[F^{t-1}, H\left(F^{t-1}\right)\right] + (1-\beta)Z^{t-1}\right\} + (1-\alpha)F^{t-1} \tag{18}$$

Fixed points $(\widetilde{Z}, \widetilde{F})$ of (17) and (18) are found by setting

$$Z^t = Z^{t-1} = \widetilde{Z} \tag{19}$$

$$F^t = F^{t-1} = \widetilde{F} \tag{20}$$

which results in the following equations:

$$\widetilde{Z} = V\left[\widetilde{F}, H(\widetilde{F})\right] \tag{21}$$

$$\widetilde{F} = S(\widetilde{Z}) \tag{22}$$

with the corresponding fixed-point green split of link 1 being given by

$$\widetilde{G} = H(\widetilde{F}) \tag{23}$$

We now turn to the derivation of conditions for fixed point local stability based on the Jacobian matrix of (17) and (18)

$$J = \begin{bmatrix} \frac{\partial Z^t}{\partial Z^{t-1}} & \frac{\partial Z^t}{\partial F^{t-1}} \\ \frac{\partial F^t}{\partial Z^{t-1}} & \frac{\partial F^t}{\partial F^{t-1}} \end{bmatrix} \tag{24}$$

whose entries are

$$\frac{\partial Z^t}{\partial Z^{t-1}} = 1-\beta \tag{25}$$

$$\frac{\partial Z^t}{\partial F^{t-1}} = \beta\left(\frac{\partial V}{\partial F} + \frac{\partial V}{\partial H}\cdot\frac{dH}{dF}\right) \tag{26}$$

$$\frac{\partial F^t}{\partial Z^{t-1}} = \alpha(1-\beta)\frac{dS}{dW} \tag{27}$$

$$\frac{\partial F^t}{\partial F^{t-1}} = \alpha\frac{dS}{dW}\beta\left(\frac{\partial V}{\partial F} + \frac{\partial V}{\partial H}\cdot\frac{dH}{dF}\right) + 1 - \alpha \tag{28}$$

where

$$W(F,Z) = \beta V[F, H(F)] + (1-\beta)Z \tag{29}$$

As stated in Section 2.1, local stability is ensured if all eigenvalues of J, evaluated at the fixed point, have a modulus smaller than 1. In the case of a two-dimensional system, this requirement can be shown to be equivalent to the following conditions:

$$D < 1 \tag{30}$$

$$D > T - 1 \tag{31}$$

$$D > -T - 1 \tag{32}$$

where D is the determinant and T is the trace of matrix J evaluated at the fixed point

$$D = (1-\alpha)(1-\beta) \tag{33}$$

$$T = 2 - \alpha - \beta + \alpha\frac{dS}{dW}\beta\left(\frac{\partial V}{\partial F} + \frac{\partial V}{\partial H}\cdot\frac{dH}{dF}\right) \tag{34}$$

Using (33) and (34), conditions (30)–(32) can be rewritten as

$$(1-\alpha)(1-\beta) < 1 \tag{35}$$

$$\frac{dS}{dW}\left(\frac{\partial V}{\partial F} + \frac{\partial V}{\partial H}\cdot\frac{dH}{dF}\right) < 1 \tag{36}$$

$$\frac{2(\alpha+\beta-2)}{\alpha\beta} - 1 < \frac{dS}{dW}\left(\frac{\partial V}{\partial F} + \frac{\partial V}{\partial H}\cdot\frac{dH}{dF}\right) \tag{37}$$

where even though not explicitly indicated, (36) and (37) are meant to be computed at the fixed point under examination.

It is immediate to check that (35) always holds because $0 < \alpha \leq 1$ and $0 < \beta \leq 1$. Expressions (36) and (37) imply that a fixed point is locally stable if

$$\frac{2(\alpha+\beta-2)}{\alpha\beta} - 1 < \frac{dS}{dW}\left(\frac{\partial V}{\partial F} + \frac{\partial V}{\partial H}\cdot\frac{dH}{dF}\right) < 1 \tag{38}$$

In the special case of "habit-free" and memoryless drivers ($\alpha = \beta = 1$), (38) reduces to

$$-1 < \frac{dS}{dW}\left(\frac{\partial V}{\partial F} + \frac{\partial V}{\partial H}\cdot\frac{dH}{dF}\right) < 1 \tag{39}$$

A comparison of expressions (38) and (39) reveals that lowering the values of α and/or β tends to widen the fixed-point stability region by decreasing its lower bound. The intuitive interpretation of this circumstance is that memory depth and inertia in route choice behavior are conducive to system stability, as they tend to reduce the day-to-day cost and flow updating rates.

The results presented above can be further specified if explicit expressions are provided for the functions involved. Before moving to this task, however, we introduce, in general terms, an explicit form of the signal control policy $\boldsymbol{H}$, which is then used in the analysis of Section 2.4.

2.3. A Logit form Signal Control Policy

Broadly speaking, a signal control policy can be defined as any method used to determine intersection signal settings as a function of vehicular flows approaching the intersection. Assuming a given layout of the control plan (number, type, and sequence of signal phases), signal settings typically consist of timing parameters such as cycle length, green splits, and possibly offsets in the case of coordinated systems. Consistent with the assumptions outlined in Section 2.2, in what follows we limit ourselves to the consideration of green splits, i.e., the phase green times expressed as fractions of the signal cycle length.

In the present study, green splits are determined according to the following expression, which has the form of the well-known Logit model

$$G_i = \frac{\exp(\gamma P_i)}{\sum_{j=1}^{N} \exp(\gamma P_j)} \qquad i = 1, \ldots, N \tag{40}$$

where

i denotes the generic phase of the signal cycle;
N represents the total number of signal phases;
G_i is the green split assigned to phase i;
P_i is the traffic pressure in phase i;
γ (> 0) is a control parameter.

We note that an expression similar to (40) for the determination of green splits has been adopted by Le et al. [37] within a different modeling framework. In general, traffic pressure is a measure of the request for capacity from vehicles moving in a given phase and can be defined in several specific forms [32]. For the purpose of the analysis presented in this study, we define pressure simply as the ratio of traffic flow to saturation flow, a quantity commonly termed flow ratio in the traffic engineering literature. The value of parameter γ, which is fully controlled by the traffic manager, determines the sensitivity of the computed green splits to the phase traffic pressures. In the limit, as $\gamma \to 0$, the cycle is evenly allocated among signal phases, regardless of traffic pressures. At the other extreme, as $\gamma \to +\infty$, the green split of the most pressurized phase tends to unity. In spite of the evident formal analogy with the effect of the dispersion parameter in the Logit route choice model, it should be noted that the latter relates to drivers' behavior, while γ is strictly a control parameter.

2.4. A Simple Specification of the Dynamic Process of Route Choice and Signal Control

In this section, we show how the analysis developed in Section 2.2 can be further specified through the definition of explicit functional forms to provide the necessary elements for the subsequent numerical tests of the dynamical system's behavior.

We assume that the travel cost functions of the two links have the following forms:

$$K_1(F, G) = a + \frac{bF}{QG} \tag{41}$$

$$K_2(F, G) = a + \frac{b(1-F)}{Q(1-G)} \tag{42}$$

where a, b are positive parameters and Q is the link saturation flow. The latter is a measure of the link's physical capacity without consideration of signal control so that the actual link capacity is obtained as the product of saturation flow and green split. Note that we assume simplified cost functions for the sake of analytical tractability of the model. More complex expressions representing in a realistic way the delay incurred by vehicles at signal-controlled intersections are adopted in the numerical tests presented in Section 4.

The share of travel demand assigned to link 1 as a function of the difference between mean perceived costs is specified through a Logit model with parameter θ as follows:

$$S(C_1 - C_2) = S(Z) = \frac{1}{1 + \exp(\theta Z)} \tag{43}$$

The green split of link 1 is determined by means of the Logit-like signal control policy introduced in Section 2.3 as follows:

$$G = H(F) = \frac{\exp\left(\frac{\gamma F}{Q}\right)}{\exp\left(\frac{\gamma F}{Q}\right) + \exp\left[\frac{\gamma(1-F)}{Q}\right]} = \frac{1}{1 + \exp\left[\frac{\gamma(1-2F)}{Q}\right]} \tag{44}$$

Subtracting (42) from (41) and substituting expression (44) for G, we obtain (see Appendix A for details)

$$V[F, H(F)] = \frac{b}{Q}\left\{F\left[\exp\left(\frac{\gamma(2F-1)}{Q}\right) + \exp\left(\frac{\gamma(1-2F)}{Q}\right) + 2\right] - \exp\left(\frac{\gamma(2F-1)}{Q}\right) - 1\right\} \tag{45}$$

If we introduce (43) and (45) into (17) and (18), the day-to-day evolution of route choice and signal control is described by the following dynamical system:

$$Z^t = \beta\frac{b}{Q}\left\{F^{t-1}\left[\exp\left(-U\left(F^{t-1}\right)\right) + \exp\left(U\left(F^{t-1}\right)\right) + 2\right] - \exp\left(-U\left(F^{t-1}\right)\right) - 1\right\} + (1-\beta)Z^{t-1} \tag{46}$$

$$F^t = \frac{\alpha}{1 + \exp[\theta W(F^{t-1}, Z^{t-1})]} + (1-\alpha)F^{t-1} \tag{47}$$

having defined

$$U(F) = \frac{\gamma(1-2F)}{Q} \tag{48}$$

$$W(F, Z) = \beta\frac{b}{Q}\{F[\exp(-U(F)) + \exp(U(F)) + 2] - \exp(-U(F)) - 1\} + (1-\beta)Z \tag{49}$$

where (49) can be recognized as being a specific instance of (29).

A fixed point of (46) and (47) is a pair $(\widetilde{Z}, \widetilde{F})$, such that

$$\widetilde{Z} = \frac{b}{Q}\left\{\widetilde{F}\left[\exp\left(-U(\widetilde{F})\right) + \exp\left(U(\widetilde{F})\right) + 2\right] - \exp\left(-U(\widetilde{F})\right) - 1\right\} \tag{50}$$

$$\widetilde{F} = \frac{1}{1 + \exp(\theta\widetilde{Z})} \tag{51}$$

In order to analyze fixed point local stability, we compute the entries of the Jacobian matrix (24) applied to (46) and (47)

$$\frac{\partial Z^t}{\partial Z^{t-1}} = 1 - \beta \tag{52}$$

$$\frac{\partial Z^t}{\partial F^{t-1}} = \beta\frac{b}{Q}\left\{\exp(-U(F)) + \exp(U(F)) + 2 + \frac{2\gamma}{Q}[(F-1)\exp(-U(F)) - F\exp(U(F))]\right\} \tag{53}$$

$$\frac{\partial F^t}{\partial Z^{t-1}} = -\alpha\theta(1-\beta)\frac{\exp[\theta W(F, Z)]}{\{1 + \exp[\theta W(F, Z)]\}^2} \tag{54}$$

$$\frac{\partial F^t}{\partial F^{t-1}} = -\frac{\alpha\beta\theta b\exp[\theta W(F,Z)]}{Q\{1+\exp[\theta W(F,Z)]\}^2}\left\{\exp(-U(F)) + \exp(U(F)) + 2 + \frac{2\gamma}{Q}[(F-1)\exp(-U(F)) - F\exp(U(F))]\right\} + 1 - \alpha \tag{55}$$

Next, we focus our analysis on the pair $(\widetilde{Z} = 0, \widetilde{F} = 0.5)$, which is a solution to (50) and (51), and we derive stability conditions for this fixed point. To this end, we note that $U(\widetilde{F} = 0.5) = 0$ and $W(\widetilde{F} = 0.5, \widetilde{Z} = 0) = 0$, so that the entries of the Jacobian evaluated at the fixed point become

$$\frac{\partial Z^t}{\partial Z^{t-1}} = 1 - \beta \tag{56}$$

$$\frac{\partial Z^t}{\partial F^{t-1}} = \frac{2\beta b}{Q}\left(2 - \frac{\gamma}{Q}\right) \tag{57}$$

$$\frac{\partial F^t}{\partial Z^{t-1}} = -\frac{\alpha\theta(1-\beta)}{4} \tag{58}$$

$$\frac{\partial F^t}{\partial F^{t-1}} = \frac{\alpha\beta\theta b}{Q}\left(\frac{\gamma}{2Q} - 1\right) + 1 - \alpha \tag{59}$$

From (56)–(59), we obtain the following expressions for the determinant D and the trace T of the Jacobian evaluated at the fixed point

$$D = (1-\alpha)(1-\beta) \tag{60}$$

$$T = 2 - \alpha - \beta + \frac{\alpha\beta\theta b}{Q}\left(\frac{\gamma}{2Q} - 1\right) \tag{61}$$

Conditions for the local stability of the fixed point under consideration can now be derived by substituting (60) and (61) into (30)–(32)

$$(1-\alpha)(1-\beta) < 1 \tag{62}$$

$$\frac{\theta b}{Q}\left(\frac{\gamma}{2Q} - 1\right) < 1 \tag{63}$$

$$\frac{2(\alpha+\beta-2)}{\alpha\beta} - 1 < \frac{\theta b}{Q}\left(\frac{\gamma}{2Q} - 1\right) \tag{64}$$

As before (see Section 2.2), we observe that (62) always holds because $0 < \alpha \leq 1$ and $0 < \beta \leq 1$. Expressions (63) and (64) imply that the fixed point is locally stable if

$$\frac{2(\alpha+\beta-2)}{\alpha\beta} - 1 < \frac{\theta b}{Q}\left(\frac{\gamma}{2Q} - 1\right) < 1 \tag{65}$$

In the special case of "habit-free" and memoryless drivers $(\alpha = \beta = 1)$, (65) reduces to

$$-1 < \frac{\theta b}{Q}\left(\frac{\gamma}{2Q} - 1\right) < 1 \tag{66}$$

Depending on the purpose of the analysis, condition (65) can be employed to determine the lower and upper limits of the fixed-point stability region in terms of any of the involved parameters for given values of the remaining ones. Note that, out of the six parameters appearing in expression (65), three (α, β, θ) represent *behavioral features* of the drivers, two (b, Q) depend on the *physical characteristics* of the network elements, and one (γ) relates to the *signal control policy* adopted by the traffic management agency. Since in the present study, the main emphasis is on the impact of the Logit-like signal setting policy on the day-to-day evolution of the network state, in what follows, we focus on the effect of parameter γ on fixed point local stability. This allows us to demonstrate how an appropriately calibrated signal control strategy has the potential to neutralize the instabilities induced by drivers' behavioral traits and network physical features.

To this end, we rewrite conditions (63) and (64) in terms of γ to obtain

$$2Q\left\{1+\frac{Q}{\theta b}\left[\frac{2(\alpha+\beta-2)}{\alpha\beta}-1\right]\right\}<\gamma<2Q\left(1+\frac{Q}{\theta b}\right) \tag{67}$$

which, in the special case $\alpha=\beta=1$, reduces to

$$2Q\left(1-\frac{Q}{\theta b}\right)<\gamma<2Q\left(1+\frac{Q}{\theta b}\right) \tag{68}$$

Note that since $\gamma>0$, the lower limit of the range shown in (67) is effectively binding if

$$2Q\left\{1+\frac{Q}{\theta b}\left[\frac{2(\alpha+\beta-2)}{\alpha\beta}-1\right]\right\}>0 \tag{69}$$

which implies

$$1+\frac{2(2-\alpha-\beta)}{\alpha\beta}<\frac{\theta b}{Q} \tag{70}$$

Similarly, the lower limit of the range shown in (68) is effectively binding if

$$2Q\left(1-\frac{Q}{\theta b}\right)>0 \tag{71}$$

which implies

$$Q<\theta b \tag{72}$$

3. Numerical Example #1: Two-Link Network

A graphical illustration of the relationships between each of the extremes of range (67) and parameter θ is provided in Figures 2 and 3 for fixed values of b and Q. Note that the upper bound γ_max is independent of the inertia and memory depth parameters α and β, and that the latter can be interchanged without affecting the value of the lower bound γ_min. We also observe that, according to condition (69), any negative value of γ_min is replaced by 0, which explains the null portions of the curves shown in Figure 3. For the same reason, the curves corresponding to low values of α and β (0.1, 0.2, and 0.3), which would be entirely replaced by null functions, are not shown in the graph.

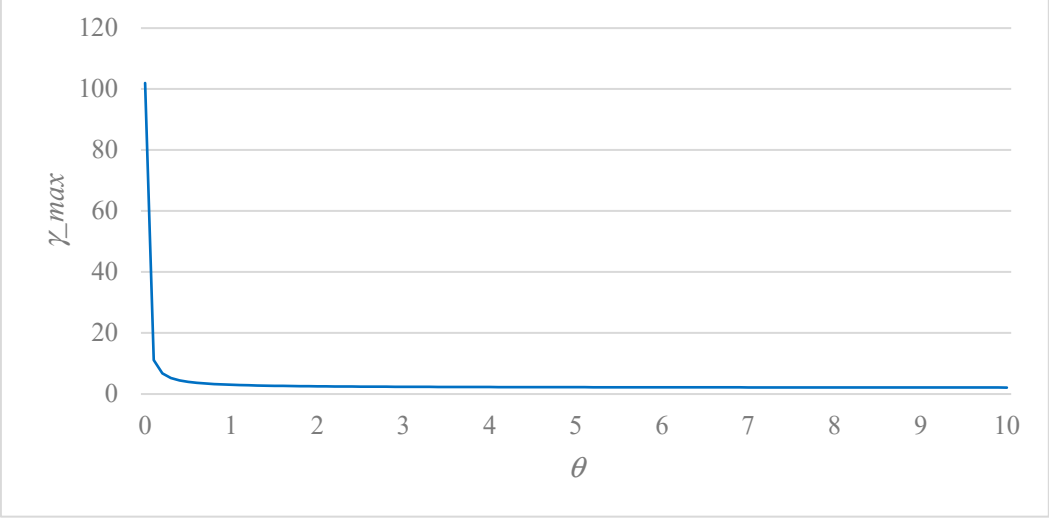

Figure 2. Maximum value of γ ensuring fixed-point stability as a function of the Logit route choice parameter θ ($b=2$; $Q=1$).

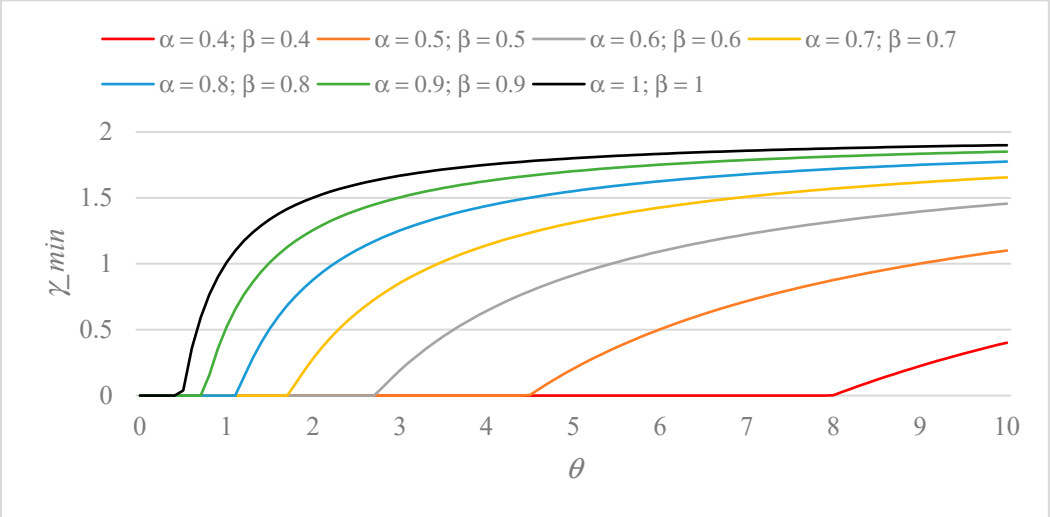

Figure 3. Minimum value of γ ensuring fixed-point stability as a function of the Logit route choice parameter θ for different values of α and β ($b = 2$; $Q = 1$).

The joint analysis of Figures 2 and 3 reveals that the range of γ values ensuring fixed-point stability tends to shrink as θ increases, and that this effect becomes more and more pronounced as α and β grow and tend to unity. From a policy standpoint (recalling that θ increases as drivers' knowledge of actual travel costs improves), this amounts to a progressive reduction of the signal timing options available to the traffic manager to offset the destabilizing effects of drivers' accurate cost perception, low inertia, and shallow memory.

The effect of the model parameters on the trajectory of the dynamical system (46) and (47) is illustrated by means of the examples displayed in Figures 4–8, which show the time evolution of F over 200 periods for different combinations of parameter values. Under conditions of local stability, the trajectory of system states may converge to the $\tilde{F} = 0.5$ fixed point either with a smooth pattern (Figure 4) or following damped oscillations (Figure 5). On the other hand, when instability prevails, the system may evolve toward a periodic (Figure 6) or an aperiodic (Figure 7) attractor, as well as toward alternate fixed points (Figure 8), unless initialized exactly at $\tilde{F} = 0.5$.

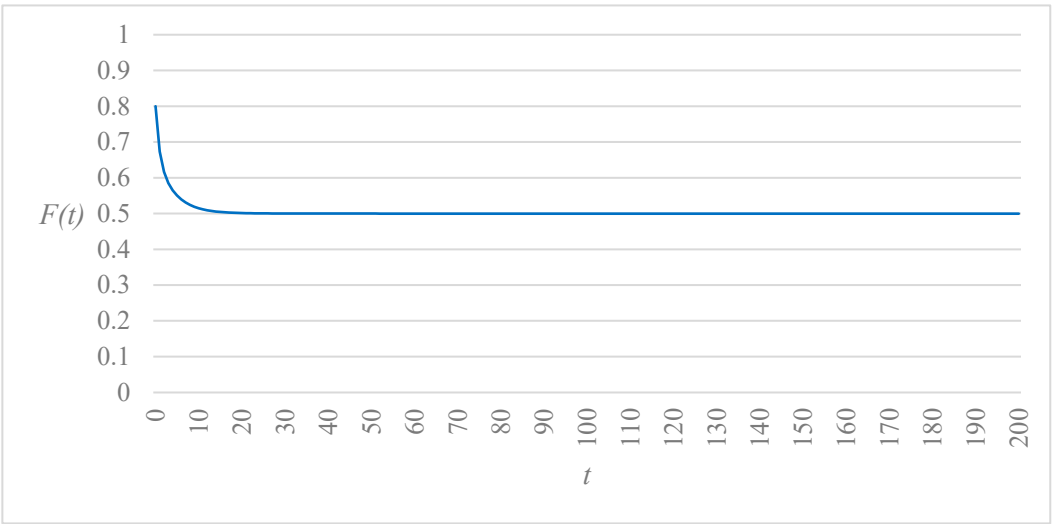

Figure 4. Time evolution of F for $\alpha = 0.6$; $\beta = 0.4$; $\gamma = 3$; $\theta = 0.5$; $b = 1.5$; $Q = 1$; $F(0) = 0.8$.

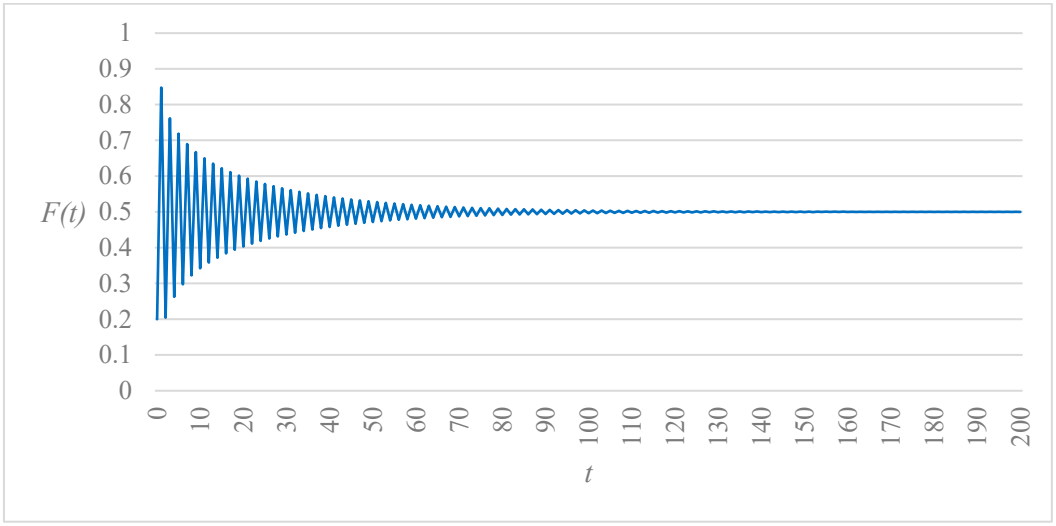

Figure 5. Time evolution of F for $\alpha = 0.9; \beta = 0.8; \gamma = 1.05; \theta = 1.5; b = 2.5; Q = 1; F(0) = 0.2$.

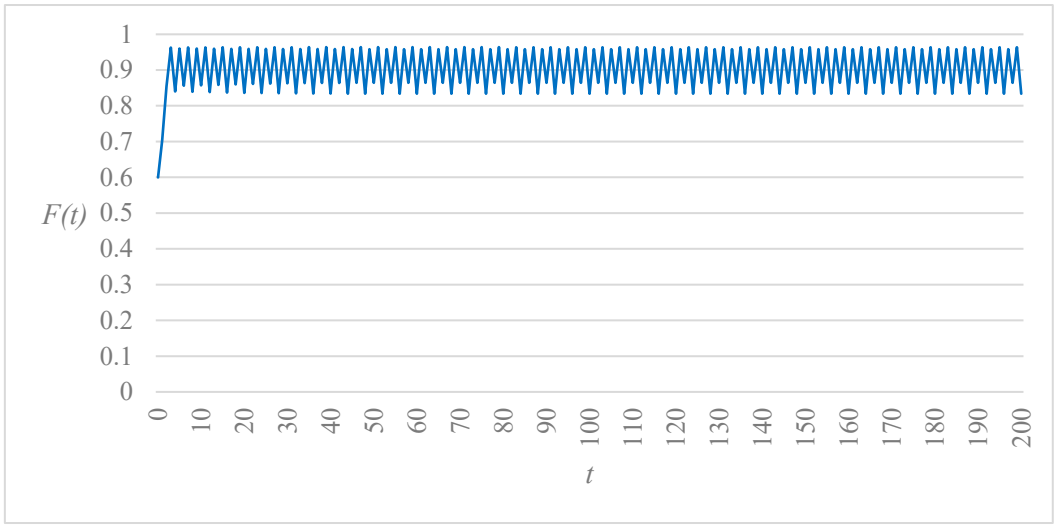

Figure 6. Time evolution of F for $\alpha = 1; \beta = 0.8; \gamma = 4.05; \theta = 1; b = 2; Q = 1; F(0) = 0.6$.

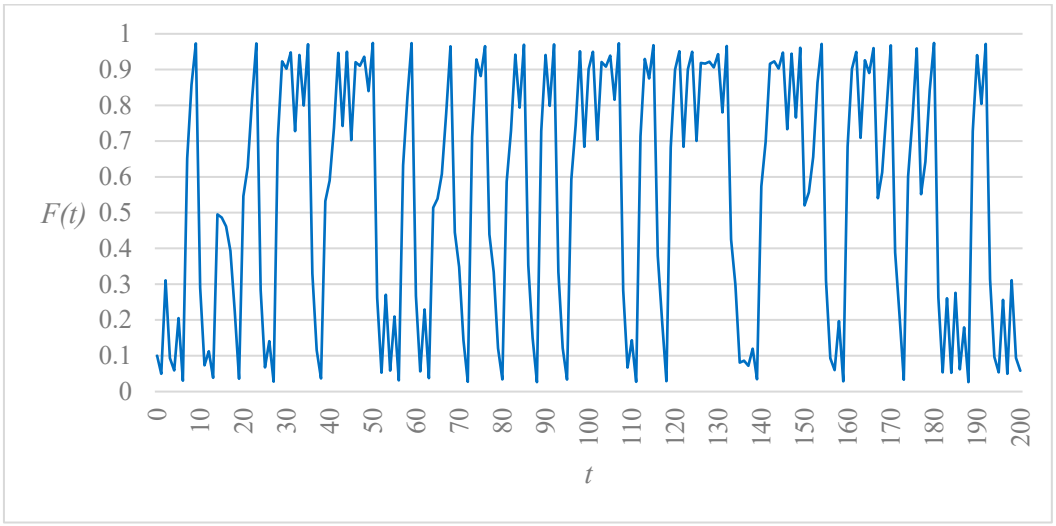

Figure 7. Time evolution of F for $\alpha = 1; \beta = 1; \gamma = 3.5; \theta = 2.5; b = 1.5; Q = 1; F(0) = 0.1$.

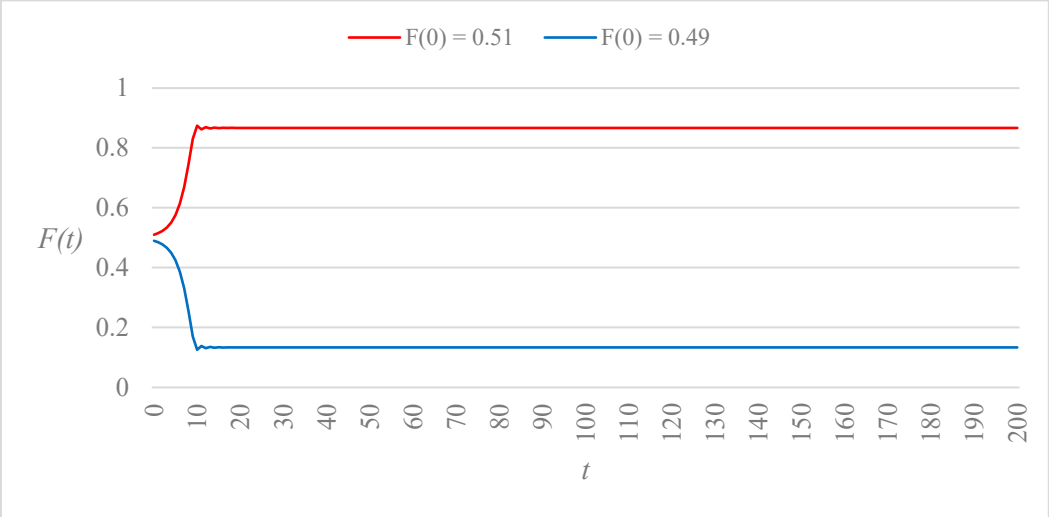

Figure 8. Time evolution of F for $\alpha = 1; \beta = 1; \gamma = 3.5; \theta = 1; b = 2; Q = 1; F(0) = 0.49; 0.51$.

4. Numerical Example #2: Grid Network

In this section, the proposed day-to-day dynamic process model of route choice and signal control is further analyzed through numerical tests carried out on the ten-link network shown in Figure 9. Three of the network nodes are assumed to represent intersections controlled by traffic signals operating on a two-phase plan with a fixed cycle of 90 s. Each of the six routes connecting the origin to the destination traverses at least one signal-controlled intersection. The functional characteristics of the ten network links are specified in Table 1. Note that the capacities of links 3–8 are determined endogenously as the product of the respective saturation flows and green splits, while those of the remaining links (1, 2, 9, and 10) are fixed exogenously.

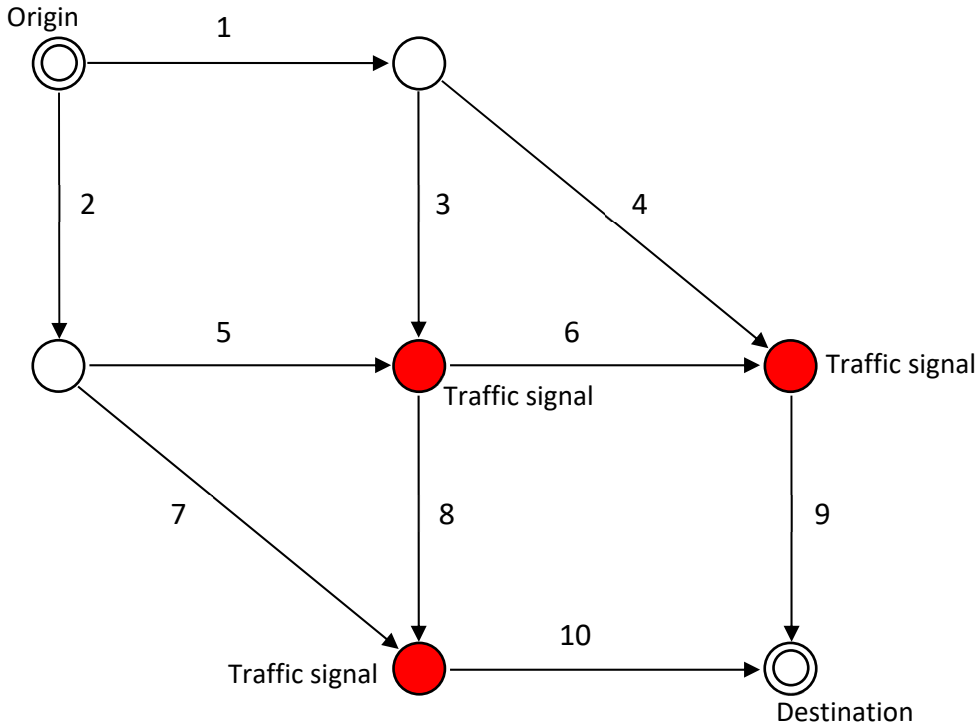

Figure 9. Grid network with three signal-controlled intersections.

Table 1. Test network data.

Link	Free-Flow Travel Time (min.)	Saturation Flow (veh./h)	Capacity (veh./h)
1	5	–	1500
2	5	–	1500
3	5	1400	–
4	12	2000	–
5	5	1600	–
6	5	1400	–
7	12	2000	–
8	5	1500	–
9	5	–	1500
10	5	–	1500

Travel times of unsignalized links are modeled by means of the classical BPR function [38] as follows:

$$T = T_0\left(1 + 0.15\, x^4\right) \tag{73}$$

where T_0 represents travel time under free-flow conditions and x is the link's flow-to-capacity ratio.

On the other hand, travel times of signalized links are computed by adding to their free-flow value a delay term representing the effect of signal control under congestion. To this end, we employ a "sheared" delay function, which extends the well-known Webster formula [39] to cover flow-to-capacity ratios greater than unity, thus accounting for the effect of temporary oversaturation on overall vehicular delay. Among the several functions of this type documented in the literature, we adopt in this study the expression commonly known as the "Canadian formula" [40]

$$\bar{d} = \frac{c(1-G)^2}{2[1 - G{\cdot}\min(x,1)]} + 900\tau\left[x - 1 + \sqrt{(x-1)^2 + \frac{4x}{\tau Q G}}\right] \tag{74}$$

where for a given signal-controlled link

$\bar{d}$ is the average overall vehicular delay (s);
c is the signal cycle length (s);
G is the green split;
x is the flow-to-capacity ratio;
τ is the duration of the arrival overflow (h);
Q is the saturation flow (veh./h).

Note that the first term of (74) coincides with the average uniform delay of Webster's formula and provides an estimate of the delay induced by the cyclic nature of the traffic signal operation. The second component of (74), instead, differs from Webster's incremental term in that it represents the delay caused by sustained oversaturation conditions in addition to the effect of "instantaneous" overflows arising from the stochastic nature of vehicular arrivals. In the numerical example described in this section, expression (74) is applied to the signal-controlled links of the test network setting $c = 90$ s, $\tau = 0.25$ h, and the saturation flow values shown in Table 1. Unlike these parameters, which are fixed exogenously, G and x are endogenous variables.

Since the analysis presented in the following focuses on the relationship between the values of γ ensuring fixed-point stability and the route choice parameter θ, the values of α and β were kept fixed in the numerical tests carried out on the grid network. According to Cantarella [41], plausible values for these parameters lie in the ranges 0.4–0.6 and 0.4–0.8, respectively; based on this indication, the midpoints of such intervals ($\alpha = 0.5$; $\beta = 0.6$) are assumed as representative values in our analysis.

Using the above-specified parameter values, the model was solved numerically by running 2000 iterations (time periods) of the dynamic process for different combinations of discrete values of θ and γ. More precisely, θ was increased with 0.05 increments starting from 0.1, and γ was changed with 0.5 increments in the range of 0.5–5. For each tested value of θ, the interval of γ values ensuring convergence to a fixed point was determined. Note that, unlike the analysis described in Section 2.4 and illustrated by example #1, the approach adopted here does not yield the exact limits of the γ stability region as a function of the route choice parameter. Nevertheless, it does provide an approximate indication of the width of such a region, which is deemed sufficient for practical purposes.

The results of the above-described computations are presented in Figures 10–12 that show, for three levels of demand (total trip rate from origin to destination), the approximate size of the γ stability interval (given by the difference γ_2–γ_1) as a function of θ. In each of the three figures, the point at which the γ_1 and γ_2 lines intersect corresponds to the value of θ beyond which no value of γ can ensure convergence to a fixed point, meaning that it is no longer possible to achieve system stability through a proper calibration of the signal control policy.

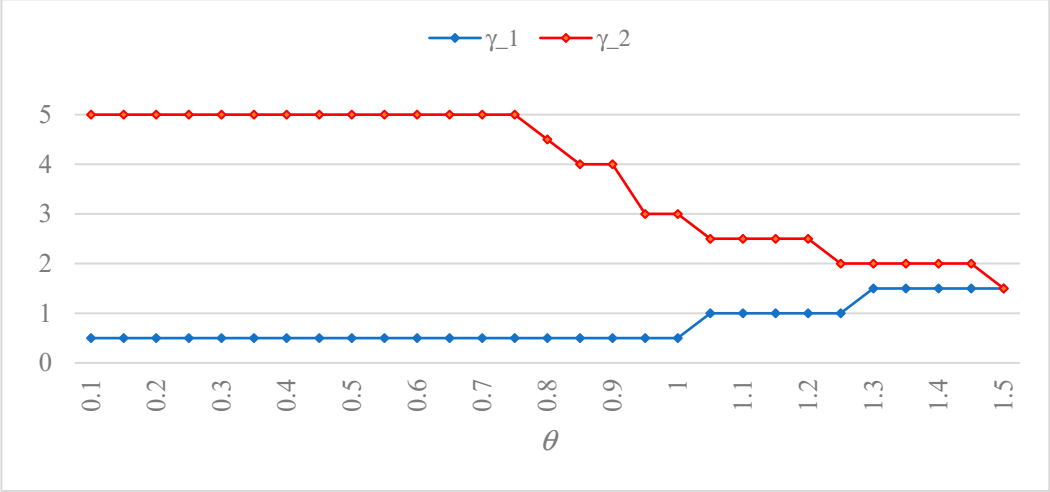

Figure 10. Approximate lower (γ_1) and upper (γ_2) limits of the fixed-point stability region in terms of γ as a function of θ (total trips = 2800 veh./h).

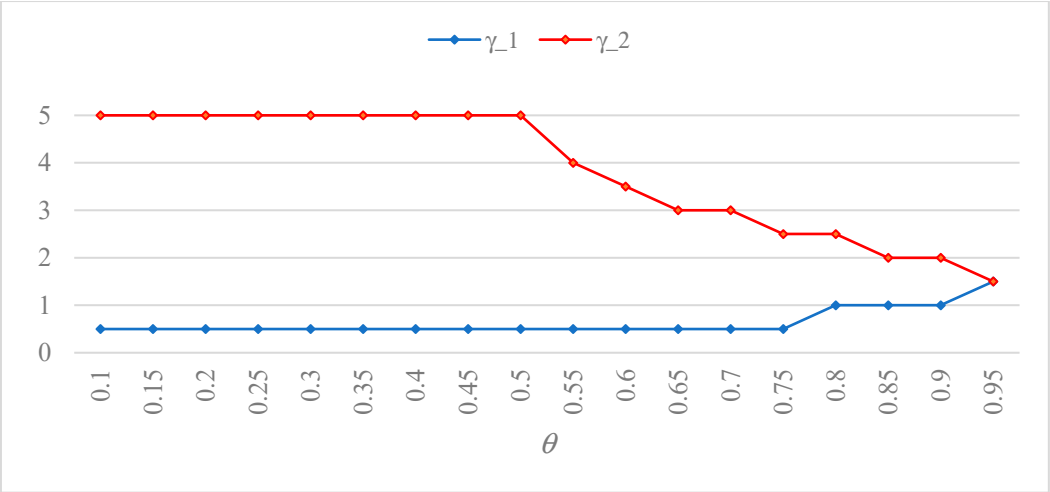

Figure 11. Approximate lower (γ_1) and upper (γ_2) limits of the fixed-point stability region in terms of γ as a function of θ (total trips = 3100 veh./h).

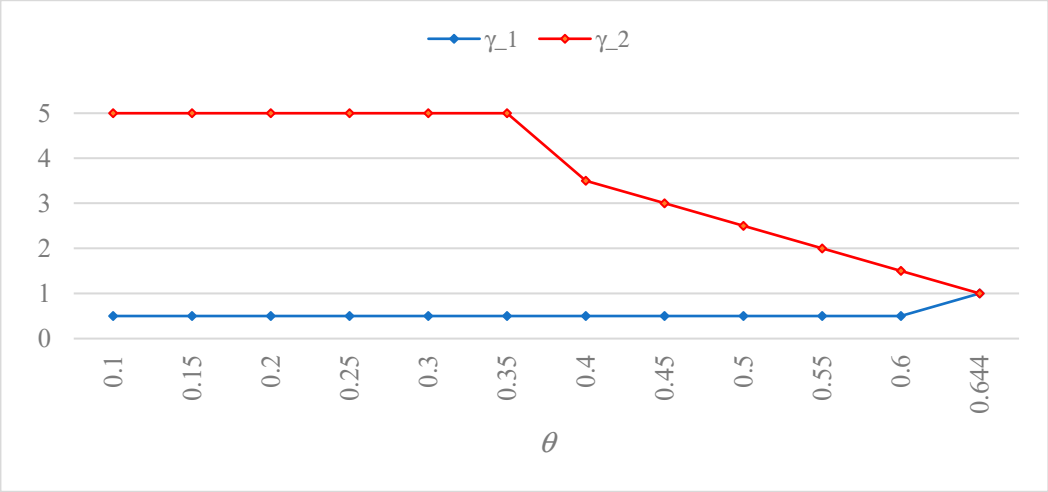

Figure 12. Approximate lower (γ_1) and upper (γ_2) limits of the fixed-point stability region in terms of γ as a function of θ (total trips = 3400 veh./h).

It is apparent in Figures 10–12 that the range of γ values ensuring fixed-point stability tends to shrink progressively as θ grows. Since θ is an increasing function of the accuracy of drivers' perception of travel times, which depends, in turn, on the available information, one may conclude that enhancing the accuracy of the information provided to users reduces the freedom available to the traffic manager in the process of calibrating a "stabilizing" signal control policy. In other words, fixed-point stability can be achieved only through a careful fine-tuning of parameter γ when drivers' information is highly accurate. From a policy standpoint, this consideration may become important when adaptive signal control is implemented jointly with Advanced Traveler Information Systems (ATISs), as the main goal of the latter is to improve drivers' knowledge of network conditions.

A comparison of Figures 10–12 further suggests that increasing travel demand reduces the size of the stability region. The intuitive explanation of this result is that it is necessary to decrease the sensitivity of route choices to costs (represented by parameter θ) in order to offset the destabilizing effect of higher congestion levels.

Finally, a comparison between the Logit-like control policy (40) and the well-known Equisaturation signal setting method [39] was carried out using average intersection delay at equilibrium as a performance metric. The latter was defined as the overall flow-weighted average of vehicular delays for all signalized links, each being computed by means of expression (74). Consistent with the previous analysis, the focus is again on the relationship between the chosen descriptor and the route choice parameter θ over the fixed-point stability region. In order to assess the effect of the demand level on the comparative performance of the two control policies, the analysis was repeated using the three values of total trip rate previously assumed for the determination of the γ stability intervals (2800, 3100, and 3400 vehicles/h.). For the Logit policy, γ was varied as before from 0.5 to 5 with 0.5 increments, and the optimal (delay-minimizing) value of this parameter was taken as representative of the policy's performance for any given value of θ. All remaining parameters were fixed at the previously used values.

The results displayed in Figures 13–15 clearly show that the Logit policy outperforms Equisaturation for all tested values of θ in each of the three demand-level scenarios. Inspection of the graphs also suggests different sensitivities of average intersection delay to the value of θ for the two policies. Moreover, it is interesting to note that the two signal setting methods perform almost equally only for the lowest values of θ. The intuitive explanation of this result is that a small value of θ implies large driver perception errors, so route choices are dominated by random effects and, hence, they are independent of actual travel times. This, in turn, means that the impact of the control strategy tends to become negligible under conditions of poor driver information.

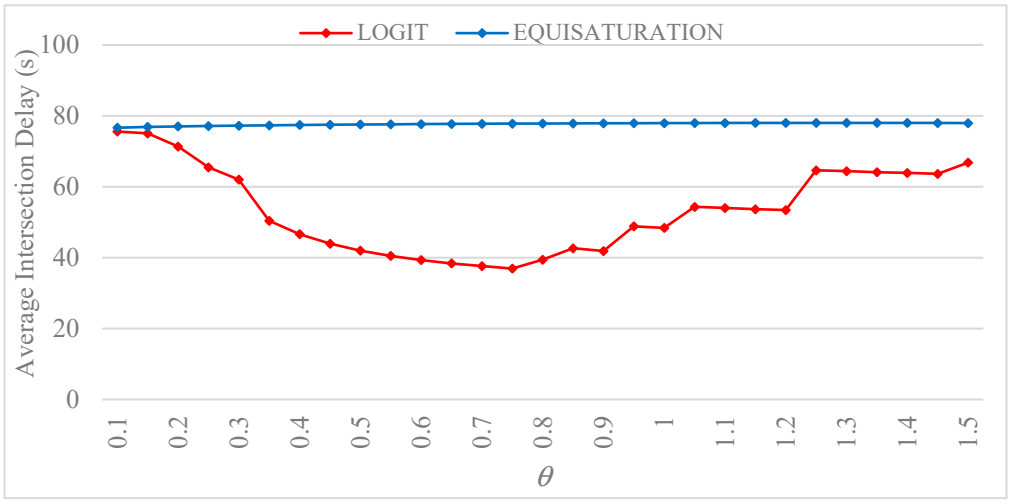

Figure 13. Average intersection delay under Logit (with optimal γ) and Equisaturation signal control policies as a function of θ (total trips = 2800 veh./h).

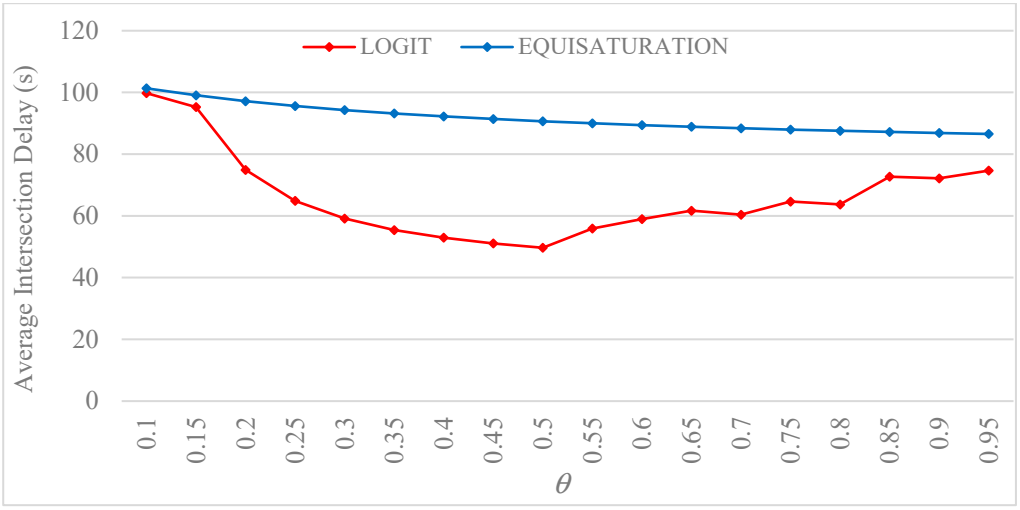

Figure 14. Average intersection delay under Logit (with optimal γ) and Equisaturation signal control policies as a function of θ (total trips = 3100 veh./h).

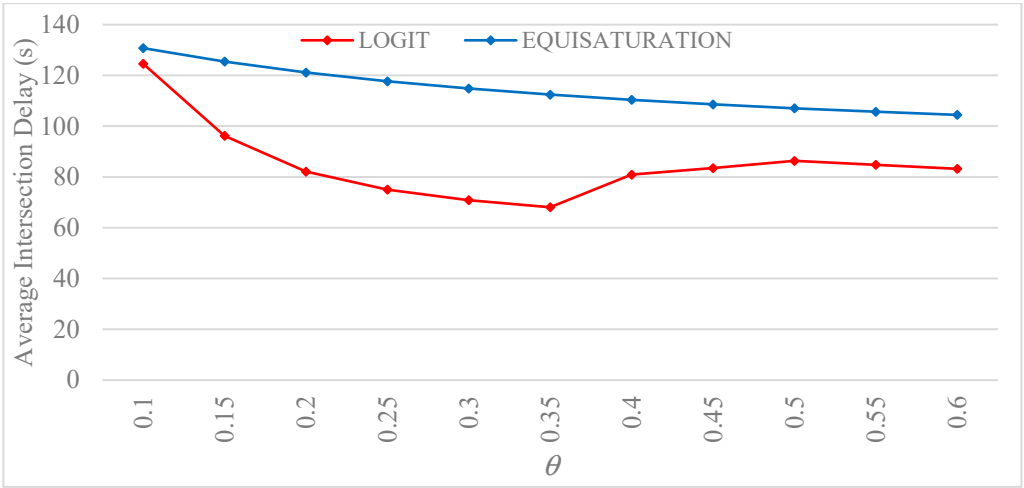

Figure 15. Average intersection delay under Logit (with optimal γ) and Equisaturation signal control policies as a function of θ (total trips = 3400 veh./h).

Since pollutant emissions and fuel consumption at intersections are closely related to vehicular delay, the results of this analysis suggest that the use of a Logit signal setting policy with a properly calibrated control parameter may also be advantageous from an environmental standpoint.

5. Conclusions

The stability of traffic equilibria in a road network with adaptive signal control is a particularly challenging issue since the responsiveness of the signal settings to route choices introduces an additional dimension into the day-to-day dynamics of the traffic system.

In this study, the joint evolution of traffic flows and adaptive signal control has been investigated by means of a nonlinear dynamical systems approach, with a specific focus on the fixed-point stability property. We have shown how a Logit form signal setting policy can be used, upon the proper calibration of the embedded control parameter, to counter the emergence of instabilities possibly arising as a consequence of various behavioral factors and network conditions.

For the sake of analytical tractability, the theoretical part of this study has addressed the very simple case of a two-route network with an intersection controlled by a two-phase traffic signal. The subsequent analysis conducted on a small but somewhat more realistic network appears to support numerically the findings emerging from the analytical investigation. Nonetheless, we are aware that more complicated scenarios in terms of network size and control strategies should be considered in future research in order to strengthen the conclusions of this study.

The findings of this research may have significant policy implications for the design and evaluation of integrated traffic management and information systems. The state of a traffic system and the long-term outcome of its dynamic evolution are the result of the interplay between a number of factors related to the physical and functional configuration of the network and to the behavioral features of the users. In general terms, stability is ensured as long as the parameters representing these factors remain within certain ranges. Since tradeoffs between the effects of the influencing factors are possible, the idea underlying the present study is that properly calibrated signal control can be leveraged to compensate for the destabilizing effect of one or more of the other system parameters.

The examples presented in this paper demonstrate, in particular, that the proposed control policy can be used, up to a certain limit, to offset the instability likely to arise in ATIS environments as a result of the dissemination of accurate traffic information and navigational advice. Our analysis also shows that the range of signal-setting options available to the traffic manager to preserve equilibrium stability may be significantly restricted by increasing levels of network congestion.

Moreover, a comparison between the Logit control policy and the Equisaturation signal setting method was carried out in this study. Although the stability regions in terms of θ appear to be the same for both policies, our results indicate that the former may be instrumental in achieving a lower average intersection delay at equilibrium. An additional advantage of the proposed policy over Equisaturation is that the embedded control parameter may be calibrated to optimize objectives other than delay minimization while preserving fixed-point stability.

Further developments of the research described in this paper should pursue the implementation of the proposed modeling approach on networks of realistic size and structure. In addition, the approach adopted in this study could be refined by introducing a rigorous delay minimization process aimed at the determination of optimal values of the control parameter γ.

The analyses presented in this paper were purposely designed to assess the parametric effect of θ on the fixed-point stability region of the combined route choice-signal control problem. However, it is envisaged that in practical applications of the proposed approach, a single value of the parameter could be of interest. Such a fixed value should be the result

of a calibration process reflecting the average level of drivers' information about travel times in the specific situation being considered.

Finally, an issue worthy of in-depth investigation is the effect of the initial state of the dynamical system on its long-term evolution. For fixed points, this analysis leads quite naturally to the problem of identifying the attraction domains of the multiple equilibria, which generally exist in models combining route choice and adaptive signal control. As shown by Xiao and Lo by means of a simple example [10], this information can be used by the traffic manager for the design of an effective signal control strategy.

Funding: This research received no external funding.

Institutional Review Board Statement: Not applicable.

Informed Consent Statement: Not applicable.

Data Availability Statement: Data used in the numerical tests are presented in Sections 3 and 4 of the article.

Conflicts of Interest: The author declares no conflicts of interest.

Appendix A. Derivation of Expression (45)

Given the travel cost functions of the two links

$$K_1(F,G) = a + \frac{bF}{QG} \tag{A1}$$

$$K_2(F,G) = a + \frac{b(1-F)}{Q(1-G)} \tag{A2}$$

we aim to express $V(F,G) = K_1(F,G) - K_2(1-F,1-G)$ as a function of F alone.

From (A1) and (A2), we have

$$V(F,G) = \frac{b}{Q}\left(\frac{F}{G} - \frac{1-F}{1-G}\right) \tag{A3}$$

According to the Logit-like signal control policy

$$G = H(F) = \frac{\exp\left(\frac{\gamma F}{Q}\right)}{\exp\left(\frac{\gamma F}{Q}\right) + \exp\left[\frac{\gamma(1-F)}{Q}\right]} = \frac{1}{1+\exp\left[\frac{\gamma(1-2F)}{Q}\right]} \tag{A4}$$

so that

$$\frac{F}{G} = F\left\{1+\exp\left[\frac{\gamma(1-2F)}{Q}\right]\right\} \tag{A5}$$

From (A4), we obtain

$$1-G = \frac{\exp\left[\frac{\gamma(1-2F)}{Q}\right]}{1+\exp\left[\frac{\gamma(1-2F)}{Q}\right]} \tag{A6}$$

so that

$$\frac{1-F}{1-G} = (1-F)\left\{\frac{1+\exp\left[\frac{\gamma(1-2F)}{Q}\right]}{\exp\left[\frac{\gamma(1-2F)}{Q}\right]}\right\} \tag{A7}$$

We now subtract (A7) from (A5) and find

$$\frac{F}{G} - \frac{1-F}{1-G} = F\left[\exp\left(\frac{\gamma(2F-1)}{Q}\right) + \exp\left(\frac{\gamma(1-2F)}{Q}\right) + 2\right] - \exp\left(\frac{\gamma(2F-1)}{Q}\right) - 1 \tag{A8}$$

which, after multiplication by (b/Q), yields expression (45) in the main text.

References

1. Allsop, R.E. Some possibilities for using traffic control to influence trip distribution and route choice. In Proceedings of the 6th International Symposium on Transportation and Traffic Theory, Sydney, Australia, 26–28 August 1974; Buckley, D.J., Ed.; Elsevier: New York, NY, USA, 1974; pp. 345–373.
2. Meneguzzer, C. Computational experiments with a combined traffic assignment and control model with asymmetric cost functions. In Proceedings of the 4th International Conference on Applications of Advanced Technologies in Transportation Engineering, Capri, Italy, 27–30 June 1995; Stephanedes, Y.J., Filippi, F., Eds.; ASCE: New York, NY, USA, 1996; pp. 609–614.
3. Meneguzzer, C. Review of models combining traffic assignment and signal control. *J. Transp. Eng.* **1997**, *123*, 148–155. [CrossRef]
4. Smith, M.J.; van Vuren, T. Traffic equilibrium with responsive traffic control. *Transp. Sci.* **1993**, *27*, 118–132. [CrossRef]
5. Meneguzzer, C. An equilibrium route choice model with explicit treatment of the effect of intersections. *Transp. Res. B* **1995**, *29*, 329–356. [CrossRef]
6. Yang, H.; Yagar, S. Traffic assignment and signal control in saturated road networks. *Transp. Res. A* **1995**, *29*, 125–139. [CrossRef]
7. Chiou, S.-W. Optimization of area traffic control for equilibrium network flows. *Transp. Sci.* **1999**, *33*, 279–289. [CrossRef]
8. Cantarella, G.E. Signal setting with dynamic process assignment. In *New Developments in Transport Planning: Advances in Dynamic Traffic Assignment*; Tampère, C.M.J., Viti, F., Immers, L.H., Eds.; Edward Elgar: Northampton, MA, USA, 2010; pp. 29–56.
9. Meneguzzer, C. Dynamic process models of combined traffic assignment and control with different signal updating strategies. *J. Adv. Transp.* **2012**, *46*, 351–365. [CrossRef]
10. Xiao, L.; Lo, H.K. Combined route choice and adaptive traffic control in a day-to-day dynamical system. *Netw. Spat. Econ.* **2015**, *15*, 697–717. [CrossRef]
11. Horowitz, J.L. The stability of stochastic equilibrium in a two-link transportation network. *Transp. Res. B* **1984**, *18*, 13–28. [CrossRef]
12. Smith, M.J. The stability of a dynamic model of traffic assignment—An application of a method of Lyapunov. *Transp. Sci.* **1984**, *18*, 245–252. [CrossRef]
13. Cantarella, G.E.; Cascetta, E. Dynamic processes and equilibrium in transportation networks: Towards a unifying theory. *Transp. Sci.* **1995**, *29*, 305–329. [CrossRef]
14. Watling, D. Stability of the stochastic equilibrium assignment problem: A dynamical systems approach. *Transp. Res. B* **1999**, *33*, 281–312. [CrossRef]
15. Watling, D.; Hazelton, M.L. The dynamics and equilibria of day-to-day assignment models. *Netw. Spat. Econ.* **2003**, *3*, 349–370. [CrossRef]
16. Bie, J.; Lo, H.K. Stability and attraction domains of traffic equilibria in a day-to-day dynamical system formulation. *Transp. Res. B* **2010**, *44*, 90–107. [CrossRef]
17. Sun, M. A day-to-day dynamic model for mixed traffic flow of autonomous vehicles and inertial human-driven vehicles. *Transp. Res. E* **2023**, *173*, 103113. [CrossRef]
18. Meneguzzer, C. Day-to-day dynamics in a simple traffic network with mixed direct and contrarian route choice behaviors. *Physica A* **2022**, *603*, 127841. [CrossRef]
19. Iida, Y.; Akiyama, T.; Uchida, T. Experimental analysis of dynamic route choice behavior. *Transp. Res. B* **1992**, *26*, 17–32. [CrossRef]
20. Selten, R.; Chmura, T.; Pitz, T.; Kube, S.; Schreckenberg, M. Commuters route choice behavior. *Games Econom. Behav.* **2007**, *58*, 394–406. [CrossRef]
21. van Essen, M.; Thomas, T.; Chorus, C.; van Berkum, E. The effect of travel time information on day-to-day route choice behaviour: Evidence from a real-world experiment. *Transp. B Transp. Dyn.* **2019**, *7*, 1719–1742. [CrossRef]
22. Meneguzzer, C. Contrarians do better: Testing participants' response to information in a simulated day-to-day route choice experiment. *Travel Behav. Soc.* **2019**, *15*, 146–156. [CrossRef]
23. Liu, S.; Guo, L.; Easa, S.M.; Yan, H.; Wei, H.; Tang, Y. Experimental study of day-to-day route-choice behavior: Evaluating the effect of ATIS market penetration. *J. Adv. Transp.* **2020**, *2020*, 8393724. [CrossRef]
24. Hu, T.-Y.; Mahmassani, H.S. Day-to-day evolution of network flows under real-time information and reactive signal control. *Transp. Res. C* **1997**, *5*, 51–69. [CrossRef]
25. Cantarella, G.E.; Velonà, P.; Vitetta, A. Day-to-Day Dynamic Network Modeling and Optimization. In Proceedings of the 2011 14th International IEEE Conference on Intelligent Transportation Systems, Washington, DC, USA, 5–7 October 2011; pp. 2086–2092.
26. Cantarella, G.E.; Velonà, P.; Vitetta, A. Signal setting with demand assignment: Global optimization with day-to-day dynamic stability constraints. *J. Adv. Transp.* **2012**, *46*, 254–268. [CrossRef]
27. Smith, M.J. Traffic signal control and route choice: A new assignment and control model which designs signal timings. *Transp. Res. C* **2015**, *58*, 451–473. [CrossRef]
28. Smith, M.J. A local traffic control policy which automatically maximises the overall travel capacity of an urban road network. *Traffic Eng. Control* **1980**, *21*, 298–302.
29. Smith, M.J. Properties of a traffic control policy which ensure the existence of a traffic equilibrium consistent with the policy. *Transp. Res. B* **1981**, *15*, 453–462. [CrossRef]
30. Liu, R.; Smith, M.J. Route choice and traffic signal control: A study of the stability and instability of a new dynamical model of route choice and traffic signal control. *Transp. Res. B* **2015**, *77*, 123–145. [CrossRef]
31. Bar-Gera, H. Traffic assignment by paired alternative segments. *Transp. Res. B* **2010**, *44*, 1022–1046. [CrossRef]

32. Smith, M.J.; Liu, R.; Mounce, R. Traffic control and route choice: Capacity maximisation and stability. *Transp. Res. B* **2015**, *81*, 863–885. [CrossRef]
33. Smith, M.J.; Iryo, T.; Mounce, R.; Satsukawa, K.; Watling, D. Zero-queue traffic control, using green-times and prices together. *Transp. Res. C* **2022**, *138*, 103630. [CrossRef]
34. He, X.; Wang, J.; Peeta, S.; Liu, H.X. Day-to-day signal retiming scheme for single-destination traffic networks based on a flow splitting approach. *Netw. Spat. Econ.* **2022**, *22*, 855–882. [CrossRef]
35. He, X.; Liu, H.X.; Peeta, S. A generalized flow splitting model for day-to-day traffic assignment. *Transp. Res. Procedia* **2015**, *9*, 56–70. [CrossRef]
36. Shang, W.-L.; Chen, Y.; Li, X.; Ochieng, W.Y. Resilience analysis of urban road networks based on adaptive signal controls: Day-to-day traffic dynamics with deep reinforcement learning. *Complexity* **2020**, *2020*, 8841317. [CrossRef]
37. Le, T.; Kovacs, P.; Walton, N.; Vu, H.L.; Andrew, L.L.H.; Hoogendoorn, S.S.P. Decentralized signal control for urban road networks. *Transp. Res. C* **2015**, *58*, 431–450. [CrossRef]
38. Bureau of Public Roads. *Traffic Assignment Manual*; U.S. Department of Commerce, Urban Planning Division: Washington, DC, USA, 1964.
39. Webster, F.V. *Traffic signal settings. Road Research Technical Paper No. 39*; H.M.S.O.: London, UK, 1958.
40. Teply, S.; Allingham, D.I.; Richardson, D.B.; Stephenson, B.W. *Canadian Capacity Guide for Signalized Intersections*, 3rd ed.; Institute of Transportation Engineers, District 7: Washington, DC, USA, 2008.
41. Cantarella, G.E. Day-to-day dynamic models for Intelligent Transportation Systems design and appraisal. *Transp. Res. C* **2013**, *29*, 117–130. [CrossRef]